Immunity
Article

A Central Nervous System-Restricted Isoform of the Interleukin-1 Receptor Accessory Protein Modulates Neuronal Responses to Interleukin-1

Dirk E. Smith,[1,*] Brian P. Lipsky,[1] Chris Russell,[2] Randal R. Ketchem,[3] Jacqueline Kirchner,[1] Kelly Hensley,[1] Yangyang Huang,[4] Wilma J. Friedman,[4] Vincent Boissonneault,[5] Marie-Michèle Plante,[5] Serge Rivest,[5] and John E. Sims[1]
[1]Department of Inflammation Research
[2]Department of Molecular Sciences
[3]Department of Protein Sciences
Amgen, Seattle, WA 98119, USA
[4]Department of Biological Sciences, Rutgers University, Newark, NJ 07102, USA
[5]Laboratory of Molecular Endocrinology, CHUL Research Center and Laval University, Sainte Foy, Quebec G1V 4G2, Canada
*Correspondence: smithde@amgen.com
DOI 10.1016/j.immuni.2009.03.020

SUMMARY

Interleukin-1 (IL-1) has multiple functions in both the periphery and the central nervous system (CNS) and is regulated at many levels. We identified an isoform of the IL-1 receptor (IL-1R) accessory protein (termed AcPb) that is expressed exclusively in the CNS. AcPb interacted with IL-1 and the IL-1R but was unable to mediate canonical IL-1 responses. AcPb expression, however, modulated neuronal gene expression in response to IL-1 treatment in vitro. Animals lacking AcPb demonstrated an intact peripheral IL-1 response and developed experimental autoimmune encephalomyelitis (EAE) similarly to wild-type mice. AcPb-deficient mice were instead more vulnerable to local inflammatory challenge in the CNS and suffered enhanced neuronal degeneration as compared to AcP-deficient or wild-type mice. These findings implicate AcPb as an additional component of the highly regulated IL-1 system and suggest that it may play a role in modulating CNS responses to IL-1 and the interplay between inflammation and neuronal survival.

INTRODUCTION

The interleukin-1 (IL-1) cytokines IL-1α and IL-1β induce cellular responses through a widely expressed receptor complex comprised of the type I IL-1 receptor (IL-1R) and the IL-1R accessory protein (AcP) (Sims, 2002). The AcP receptor subunit is also used by the IL-1F6, IL-1F8 and IL-1F9, and IL-33 receptors (Ali et al., 2007; Chackerian et al., 2007; Palmer et al., 2008; Towne et al., 2004). Ligation of the IL-1 receptor complex leads to recruitment of intracellular signaling molecules mediated by conserved cytoplasmic Toll-IL-1R (TIR) domains. These signaling events underlie IL-1's ability to regulate host defense and tissue homeostasis in virtually every organ of the body. The excessive or prolonged action of IL-1, however, can lead to destructive inflammation and contribute to disease. IL-1 has been shown to play a causative or contributing role in hereditary fever syndromes, gout, rheumatoid and systemic-onset juvenile arthritis, and type II diabetes, and there are strong suggestions of involvement in osteoarthritis, ischemia-reperfusion injury, neuropathic and inflammatory pain, and Alzheimer disease. Consequently, multiple mechanisms have evolved to regulate IL-1 activity. IL-1 is strongly induced at the transcriptional level in response to innate inflammatory stimuli, and the processing of IL-1β protein from precursor to active form and its secretion from the cell are regulated processes. Subsequent to the generation of mature, active IL-1, signaling can be attenuated by an inactive ligand analog (IL-1ra) and an inhibitory soluble receptor (IL-1R type 2). The latter acts by decoying not only the IL-1 cytokine but also the essential receptor subunit, AcP (Sims and Smith, 2003). Here, we describe an additional, more subtle form of regulation. We have found a splice variant of AcP, termed AcPb, which is expressed in a CNS-specific manner and which interferes with some, but not all, IL-1 activities and thus modulates the effects of IL-1 in the brain.

RESULTS

Discovery of an IL-1R AcP Splice Isoform with a Variant TIR Domain

We identified an open reading frame in human genomic DNA sequence with similarity to members of the IL-1R family. Subsequent cloning of the full-length cDNA from both human and mouse revealed an isoform of AcP that we have termed AcPb. Figure 1A illustrates the alternative splicing by which the prototypical AcP C-terminal exon 12 is skipped and the identified exon is utilized. Shown in Figure 1B is a sequence alignment of the polypeptides encoded by exons 11–12 from AcP and the AcPb isoform. The C terminus encoded by exon 12b in AcPb has only 35% amino acid identity with that encoded by the classic AcP exon 12. It shares motifs, however, such as box 3 (FWK) that are conserved in all TIR domains. In addition, AcPb exon 12b encodes approximately 140 amino acids of additional sequence C-terminal to the TIR domain that has no homology to other protein sequences and is of unknown function.

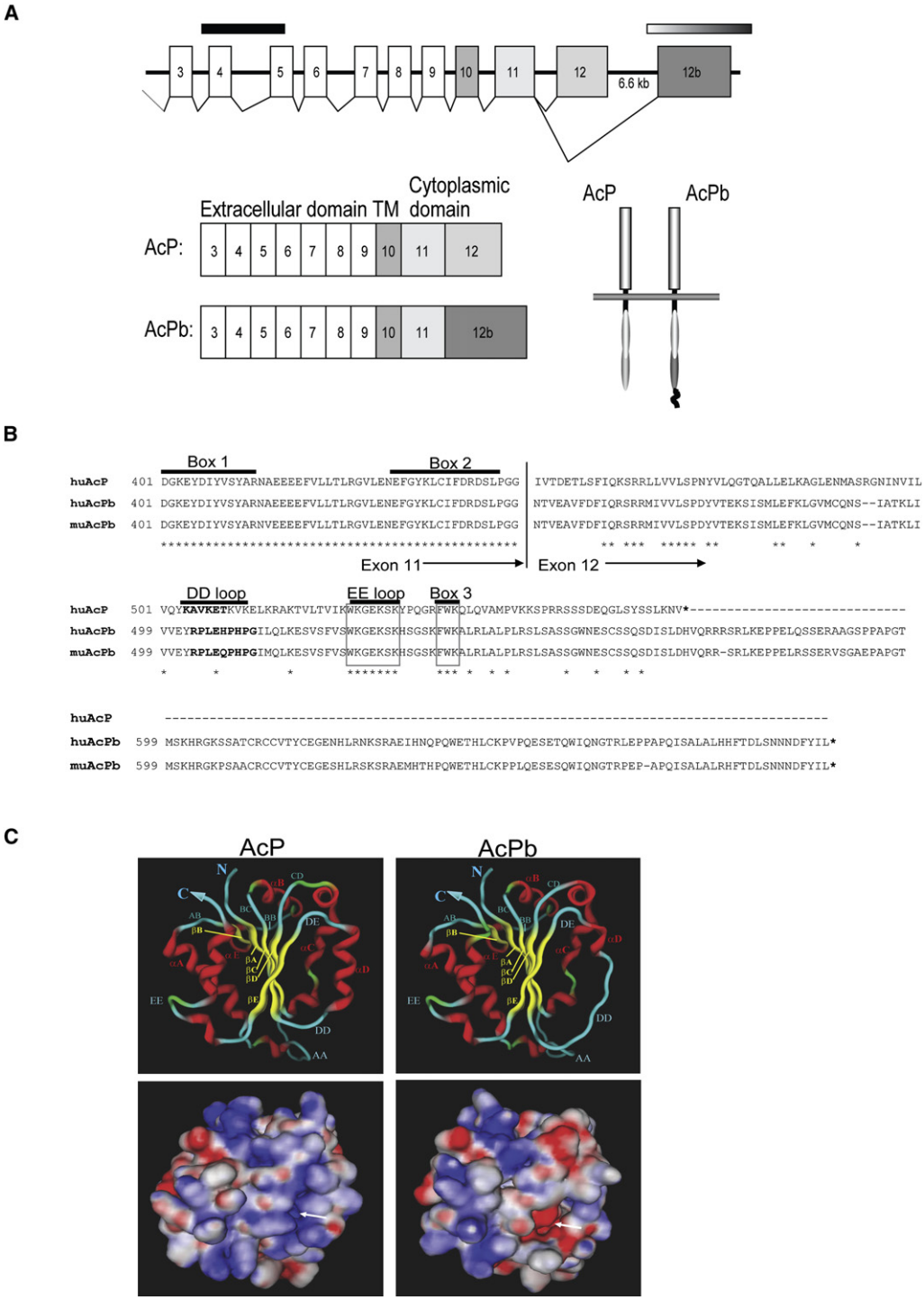

Figure 1. Genomic Organization, Sequence, and TIR Domain Structural Models of AcP Isoforms

(A) Intron-exon map of human AcP locus and alternative splicing that leads to mRNA isoforms. Shown are the translated exons (3–12) that encode the mature AcP protein. The solid black bar indicates the extracellular exons that are deleted in the AcP-deficient animals (Cullinan et al., 1998) and the faded bar indicates the specific exon 12b that is deleted in AcPb-deficient animals.

(B) Alignment of the alternative C termini of AcP and AcPb isoforms. Stars indicate conserved residues between human AcP and human AcPb. Specific structural or signaling-associated motifs are indicated.

(C) Computational models of AcP and AcPb TIR domains. Structural folds of the ribbon structure are labeled according to the convention of Khan et al. (2004). Beta sheets are indicated in yellow, alpha helices in red, and loops in blue. Shown on the bottom is the identical view with predicted surface electrostatics. Full red is equivalent to −40 kcal/mol negative charge; full blue is equivalent to 40 kcal/mol positive charge, and white is neutral charge. The arrow indicates the region of substantial charge difference caused by the disruption of the αD helix in AcPb.

Crystal structures have been determined for the TIR domains of TLR1 and TLR2 (Xu et al., 2000) as well as the orphan IL-1R family member IL-1RAPL (Khan et al., 2004). We used the latter on which to model the TIR domains of AcP and AcPb and adopted the same convention for annotation of secondary structure. The AcP TIR domain (amino acids 401–553) was predicted to contain a central 5-stranded beta-sheet surrounded by 5 alpha-helices (Figure 1C). The AcPb sequence was easily modeled onto the same structure and was remarkably similar to that of AcP, including conservation of the EE loop (approximately amino acids 527–534), previously implicated as an important site for MyD88 recruitment (Li et al., 2005; Radons et al., 2003). The only marked predicted difference between AcP and AcPb is the disruption of the αD helix in AcPb, predominantly because of two proline substitutions at amino acids 508 and 510. Predicted electrostatics indicated a more negatively charged surface on the face of the AcPb TIR domain made up of the βE strand and the DD loop-αD helix region, as a consequence of the disruption of the helix (Figure 1C, bottom). Overall, the computational modeling indicated that the AcPb cytoplasmic domain likely folds as a TIR domain similar to AcP, but with one area of substantial difference.

AcPb Expression Is Restricted to the CNS

RNA expression profiling demonstrated that whereas human *AcP* is expressed in numerous tissues, the expression of the *AcPb* isoform is much more restricted to tissues derived from the CNS (whole brain, fetal brain, cerebellum, and spinal cord) and is the more abundant isoform in these CNS tissues, with the exception of spinal cord (Figure 2A). AcPb message was undetectable or present at extremely low amount in multiple non-CNS-derived cell types and in various established cell lines including those of CNS origin, such as numerous glioblastoma and neuroblastoma-derived lines (not shown). Bronchial epithelial cells were the only non-CNS sample in which AcPb mRNA was detected; however, the expression was 1% lower than AcP mRNA and approximately 3% of the relative amount of AcPb mRNA in total brain RNA (not shown). The CNS-predominant expression pattern of *AcPb* was also observed among mouse tissues and cell lines (not shown). We next profiled the relative expression of AcP and AcPb mRNA across multiple anatomical regions of human adult brain. For comparison, the same analysis was done for mRNAs encoding both the neuron-specific gene, microtubule-associated protein 2 (MAP2), and the astrocyte-specific gene, glial fibrillary acidic protein (GFAP). *AcP* and *AcPb* have slightly different patterns of relative brain expression (Figure 2B). For example, *AcP* was much more enriched in the corpus callosum than *AcPb*, coincident with primarily glial cell bodies in this region. The AcPb mRNA expression pattern was more similar to that of MAP2 mRNA than that of GFAP mRNA, suggesting a more neuronal-restricted expression pattern. RT-PCR analysis of purified neurons, microglia, and astrocytes also indicated a more neuron-restricted expression of AcPb mRNA, whereas abundant AcP mRNA was detected in all three cell types (Figure 2C and not shown). In situ RNA hybridization was used to examine the location of expression in adult mouse brain sections with RNA probes specific for *AcP* or *AcPb* exon 12. AcP and AcPb mRNA displayed overlapping patterns of expression that corresponded to areas of neuronal bodies throughout the gray matter (Figure 2D). Collectively, these results suggest neuronal expression of AcPb throughout the brain. The mouse in situ hybridization data and RT-PCR results might suggest that AcP and AcPb are coexpressed in the same cells, rather than being expressed in different cells in the same anatomical areas, but we have been unable to raise the appropriate antibodies to prove this.

AcPb Associates with IL-1R in an IL-1-Dependent Manner

The AcPb variant conserves the extracellular domain required for interaction with IL-1R and IL-1, so we asked whether AcPb is able to form complexes with the type I IL-1R in a ligand-dependent manner. We utilized the IL-1R-positive, AcP-negative mouse T cell line EL4.16a (EL4) that was stably transduced with either a control protein (GFP) or full-length AcP or AcPb. The surface expression of reconstituted AcP or AcPb was found to be similar in both lines (Figure 3A). IL-1R was coimmunoprecipitated from both the AcP and AcPb-expressing lines but not in the control cells that lack AcP (Figure 3B, lanes 1–3). Moreover, the recruitment of IL-1R was dependent on ligation with IL-1 as shown by the fact that no IL-1R band was detected in the lanes from nontreated cells (Figure 3B, lanes 4–6). Immunoblotting with an AcP antibody confirmed that AcP and AcPb were both effectively immunoprecipitated even in the absence of IL-1. These results indicated that AcPb is capable of forming a ligand-dependent complex with IL-1R.

The proximal events that lead to IL-1-induced cellular responses involve the recruitment of specific adaptor and signaling molecules to the IL-1R:AcP complex. Two such molecules previously shown to be crucial for elicitation of IL-1 responses are the adaptor molecule MyD88 and the kinase IRAK4 (Burns et al., 2003; Huang et al., 1997; Jiang et al., 2003; Wesche et al., 1997a). Immunoprecipitation experiments with the IL-1-treated EL4 lines demonstrated that only the AcP-expressing cells are capable of recruiting MyD88 and IRAK4 after stimulation with IL-1 (Figure 3C). Although AcPb was able to associate with IL-1R under these IL-1-dependent conditions, it did not lead to the recruitment of these adaptor molecules.

AcPb Is Unable to Mediate Canonical IL-1 Signaling Responses in EL4 Cells

Experiments were next performed to determine whether AcPb possesses autonomous signaling capacity in response to IL-1 in the mouse EL4 cells. AcP-reconstituted, but not AcPb-reconstituted, cells secreted IL-2, IL-5, and IL-6 in response to IL-1 treatment (Figure 4A). In separate experiments, and consistent with previously reported results (Wesche et al., 1997b), the AcP-negative control EL4 cells were nonresponsive to IL-1, demonstrating that these responses are AcP dependent (not shown). The inability of AcPb to mediate IL-1-induced cytokine release was next shown to correspond to an inability to activate IL-1 signaling. IL-1 treatment led to the activation of the kinases p38, JNK, and ERK in the cells reconstituted with AcP, but not in the cells reconstituted with AcPb (Figure 4B). Sorbitol has previously been shown to induce p38 activation (Alpert et al., 1999) and when used as a control stimulus, it led to activation of phosphorylated p38 in all three EL4 lines, indicating that AcPb expression does not lead to a general defect in cellular responsiveness,

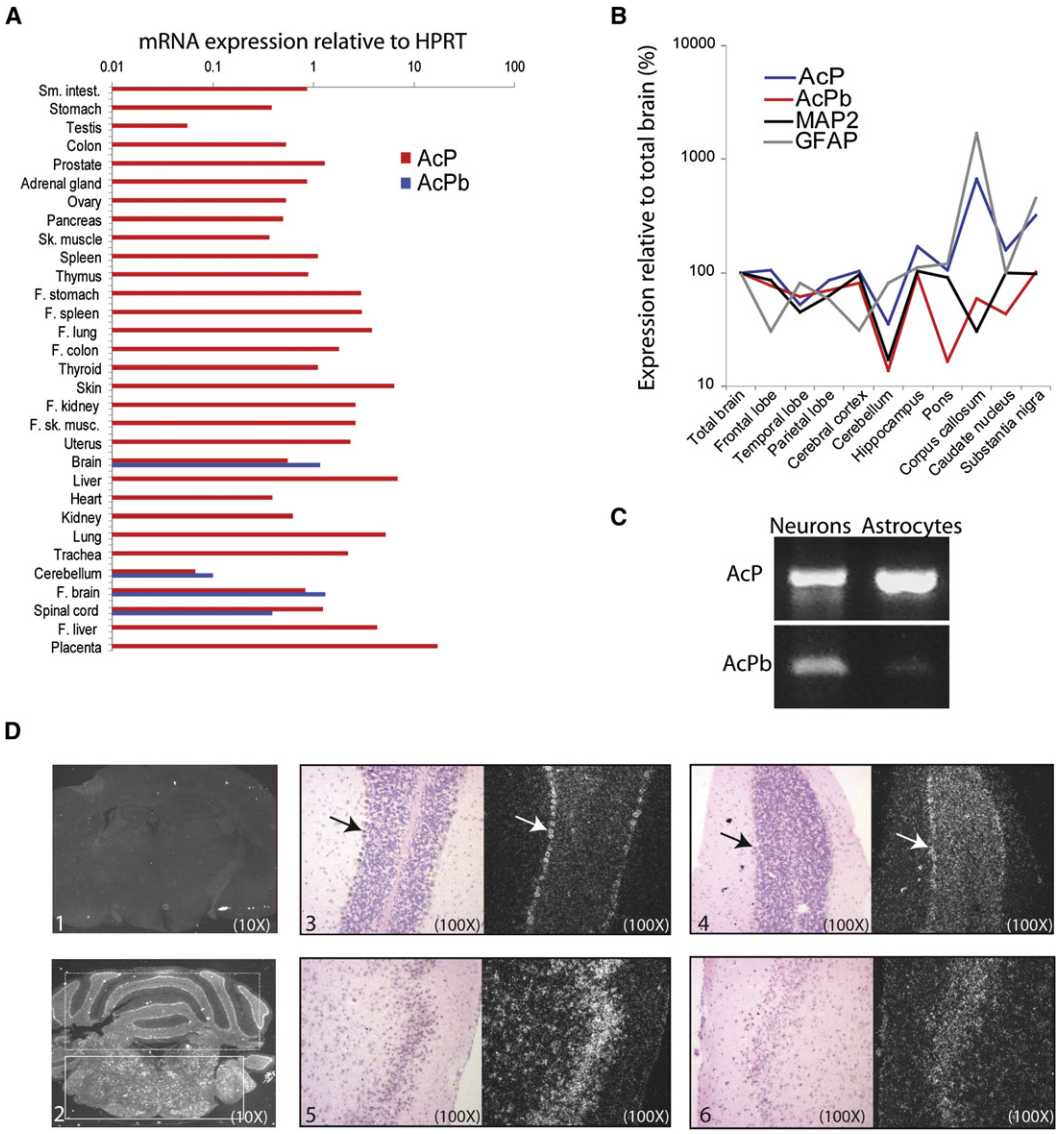

Figure 2. mRNA Expression Profile of AcP and AcPb

(A) Relative mRNA expression of AcP and AcPb isoforms in human tissues as determined by real-time PCR and presented as expression relative to HPRT. Abbreviations: F, fetal; sm, small; sk, skeletal.

(B) Normalized relative expression of AcP and AcPb mRNAs across isolated human brain regions as compared to a neuronal- and astrocyte-specific mRNA (MAP2 and GFAP, respectively). Relative expression (to HPRT) for each gene in each region was normalized to its overall expression in total brain (set to 100%).

(C) RT-PCR amplification of AcP and AcPb mRNAs from primary mouse hippocampal neuron and astrocyte cultures.

(D) In situ hybridization of section through the brainstem and cerebellum of adult mouse brain with RNA probes specific for AcP or AcPb isoforms. 1: whole brain hybridized with sense strand control probe. 2: whole brain hybridized with AcP antisense probe. Cerebellum is indicated with dashed box and the brain stem with a solid box. 3, 4: Bright field and dark field images of cerebellum hybridized with either AcP (3) or AcPb (4) antisense probes. Positively hybridizing Purkinje cells are indicated with an arrow for both probe sets. 5, 6: Bright field and dark field images of forebrain hybridized with either AcP (5) or AcPb (6) antisense probes. Positively hybridizing neuronal cell bodies are visible with both probes.

but rather, consistent with an inability to recruit MyD88 and IRAK4, is unable to mediate these specific IL-1 responses.

AcPb Effects on Gene Expression in Virally Reconstituted AcP-Deficient Cortical Neurons

We hypothesized that because the expression pattern of AcPb suggests a centrally localized function, AcPb-dependent IL-1 responses may manifest only in a CNS-related context. For example, AcPb may utilize adaptor molecules possessing the same restricted tissue expression as AcPb itself. We used a primary neuron culture system to explore this hypothesis. Cortical neuron cultures were established from C57BL/6 E17-E18 embryos and after 7–10 days the cultures were approximately 70%–80% pure MAP2-positive neurons with active neurite outgrowth (Figure 5A). Some glial cells, including GFAP-positive cells, were also present and represented

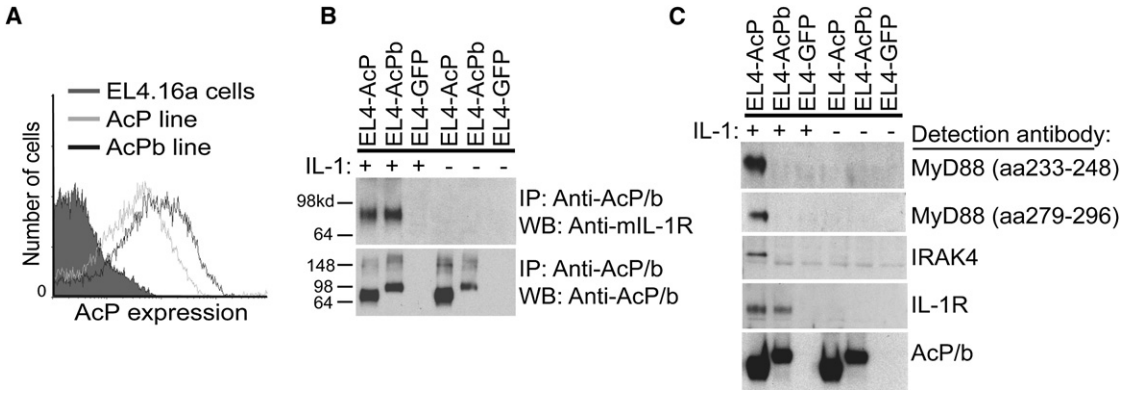

Figure 3. AcPb-Mediated IL-1R and Adaptor Recruitment

(A) AcP surface expression on EL4.16a parental and stably transfected cell lines utilizing an AcP antibody that recognizes both forms of the receptor.

(B) EL4 lines were incubated with IL-1β (100 ng/ml) for 3 min then lysed and immunoprecipitated with a pan-AcP monoclonal antibody. Precipitations were analyzed by immunoblot (WB) via either an muIL-1R antibody or a pan-AcP antibody. Approximate molecular weights are indicated.

(C) Samples were stimulated and immunoprecipitated as in (B) and then adaptor protein recruitment was determined by immunoblot with MyD88 or IRAK4 antibodies, as indicated. Data representative of duplicate independent experiments.

approximately 20%–30% of the culture. RT-PCR indicated that IL-1R, AcP, and AcPb were all expressed in these cultures and all seemed to increase in expression as the cultures matured (not shown). In order to evaluate the specific contribution of AcP (encoded by *Il1rap* gene) and AcPb toward responses to IL-1, reconstitution experiments were performed with neuronal cultures from *Il1rap*$^{-/-}$ (AcP null) E17.5 embryos. The *Il1rap*-targeted deletion eliminates two exons in the extracellular domain of AcP (as shown in Figure 1A) and thus destroys the expression of all functional AcP isoforms (Cullinan et al., 1998). Based on the previously shown ability of lentivirus to infect nondividing neurons (Blomer et al., 1997), cortical neurons from *Il1rap*$^{-/-}$ embryos were transduced in triplicate with lentiviral vectors expressing full-length AcP, AcPb, or CD25 as an unrelated control protein. A fourth population was transduced with equal amounts of both the AcP and AcPb vector in order to evaluate the effect of isoform coexpression. The infection conditions were shown to lead to vector-driven gene expression in neurons (not shown) and we presume that cotransfection occurred at the cellular level, but we are unable to rule out the possibility that some cells were only transfected with either construct alone. Two days after infection, cultures were stimulated with IL-1β for 4 or 16 hr and total RNA was harvested. RT-PCR analysis confirmed the reconstituted expression of specific receptor isoforms in each population (Figure 5B). Moreover, functional responsiveness was demonstrated by an IL-1-dependent increase in *Ccl2* expression in AcP-reconstituted cultures (Figure 5C).

In order to broadly survey the gene expression profiles of each of the IL-1-stimulated populations, RNA samples were analyzed on microarray chips containing approximately 45,000 gene probe sets. In the *Il1rap*$^{-/-}$ cultures (control virus-transduced), when comparing untreated samples to IL-1-stimulated samples at either 4 or 16 hr, the observed gene expression changes were at the level of statistical noise, consistent with the AcP requirement for IL-1 signaling (Figure 5D). In contrast, many genes were induced in the AcP-reconstituted cultures stimulated with IL-1. Statistically significant ($p < 0.05$) gene expression ratios for IL-1-treated versus untreated sample sets ranged from 1- to 2-fold up to 100-fold (the limit of the analysis dynamic range) and the specific genes regulated largely overlapped when comparing the 4 and 16 hr data sets (not shown). There was also substantial overlap between the IL-1-induced genes in the AcP-reconstituted culture and genes induced by IL-1 in a previous study with wild-type C57BL/6 cortical neurons (not shown), suggesting that transduced AcP mediated normal responses to IL-1 in this system. Some of the most robustly induced genes included chemokines such as *Cxcl1*, *Cxcl10*, and *Ccl2*, as well as immune-related products such as *Tlr2* and *Tnfrsf12a* (Table S1 available online). In contrast to the AcP-reconstituted culture, there were no genes consistently induced greater than 2-fold in the AcPb-reconstituted culture (Table S2). Moreover, the few gene responses that reached statistical significance in AcPb samples were generally induced to similar levels in the AcP-reconstituted cultures. These results indicated that AcPb-reconstituted neuronal cultures may be capable of a limited IL-1 signaling response, although all of the gene responses were modest and none were unique to AcPb.

Analysis of the AcP + AcPb-reconstituted culture compared to AcP alone indicated that AcPb coexpression was capable of modulating AcP-dependent responses. A few genes showed slightly increased induction in the AcP + AcPb-reconstituted culture as compared to AcP alone, but all of the most highly induced transcripts were induced to similar levels in the culture with AcP alone, supporting the idea that no strong gene induction signal is specifically transduced through AcPb. Interestingly, there were two classes of AcP-dependent gene responses: those that were unaffected by AcPb coexpression (example: *Gbp2* fold induction at 4 hr: AcP population, 36.8, AcP + AcPb population, 38.5) and those that were attenuated in the presence of AcPb (example: *Atf3* fold induction at 4 hr: AcP population, 22.4, AcP + AcPb population, 3.8). A summary of representative genes in both of these classes is shown in Table 1. These results suggest that in the context of a neuronal culture, AcPb coexpression may downmodulate some but not all AcP-dependent IL-1 responses.

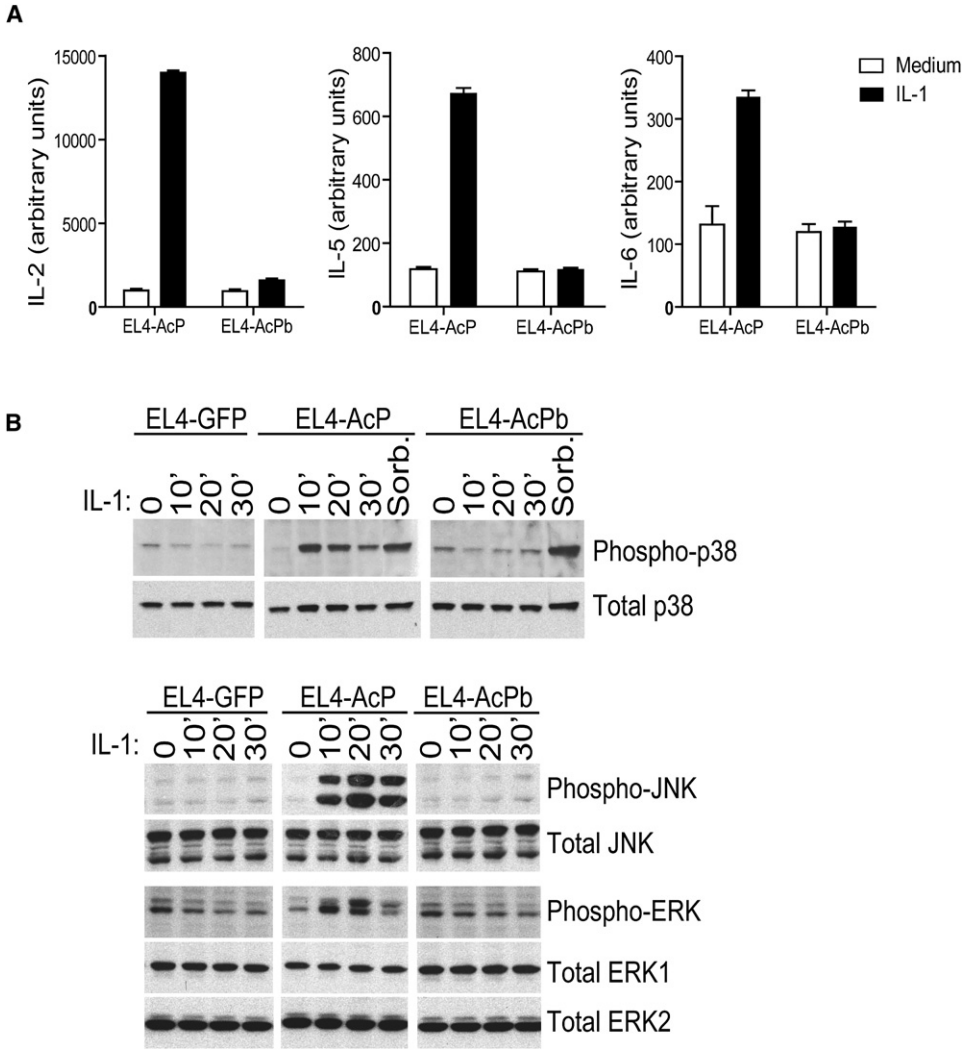

Figure 4. Signaling Capacity of AcPb-Reconstituted EL4 Cells

(A) EL4 lines were incubated for 24 hr in the presence of 300 ng/mL ionomycin and 100 pg/mL PMA plus or minus IL-1β (100 pg/mL), as indicated. Cytokine concentrations in the supernatants were quantified by Luminex (bead)-based multiplex assay and all assays were performed in triplicate. Graphs show mean plus standard deviation, n = 2.

(B) 2.0×10^7 cells were incubated with IL-1β (10 ng/mL) or 0.5 M sorbitol at 37°C for various lengths of time and lysates (approximately 0.4×10^6 cell equivalents/lane) were probed by immunoblot with total and phospho-specific antibodies against p38, JNK, and ERK, as indicated. Data representative of duplicate independent experiments.

Generation of AcPb-Deficient Mice

In order to better understand the specific function of the AcPb isoform, we generated AcPb exon 12b-deficient mice. A targeting vector was designed to delete only the unique exon 12b of the AcPb isoform while leaving all of the coding exons for classical AcP intact, as indicated in Figure 1A. Homozygous knockout animals were generated and backcrossed completely onto a C57BL/6 background. Expression of both AcP and AcPb mRNA was detected in wild-type whole brain whereas, as expected, both were absent in brains from AcP-deficient animals (Figure 6A). In contrast, only AcPb mRNA expression was disrupted in the brain of AcPb-deficient mice. At the protein level, multiple AcP-related bands were detected in wild-type brain by immunoprecipitation and immunoblotting, including bands corresponding to full-length AcP and the slightly larger AcPb (Figure 6B). We also detected smaller-sized bands, possibly corresponding to the soluble AcP mRNA variant that we have confirmed is expressed in the brain at the RNA level (not shown); however, proteomic analysis would be required to verify their identity. Control immunoprecipitations were performed with lysates from AcP- and AcPb-expressing EL4 cells. It is not clear why the receptors did not migrate exactly as the proteins in lysates from transfected EL4 cells, but differential glycosylation may underlie some of this difference. The larger AcPb-sized band was uniquely absent in the brains from AcPb-deficient mice, indicating that the exon 12b deletion resulted in loss of this isoform but did not interfere with protein expression of the other forms of AcP.

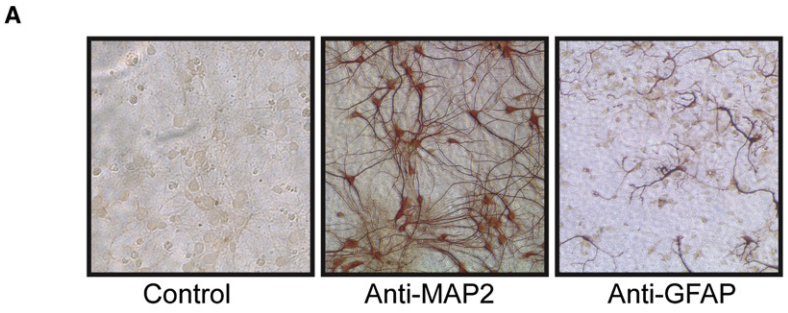

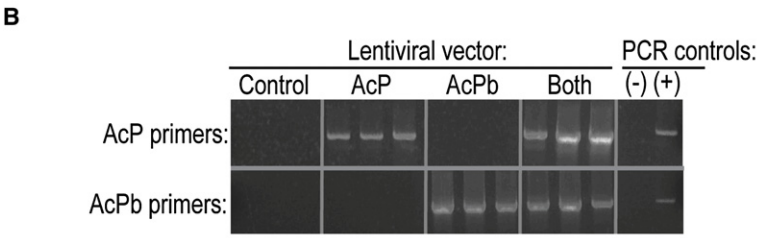

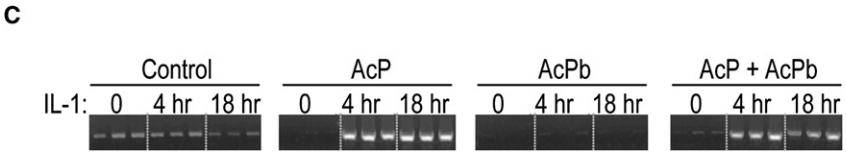

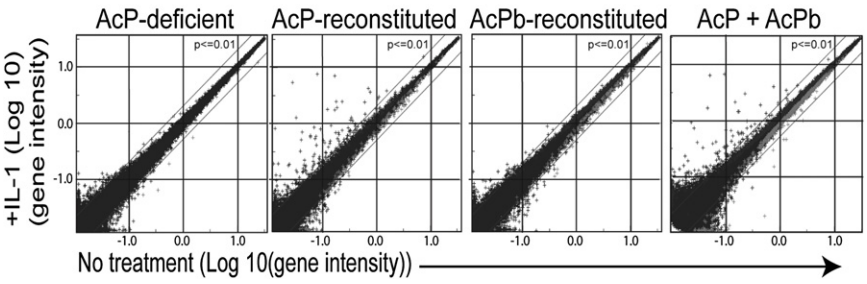

Figure 5. IL-1-Induced Responses in Primary Cortical Neurons

(A) C57BL/6 embryonic cortical neuron cultures were stained by immmunohistochemistry after 9 days of culture with antibodies that recognize either the neuronal-specific protein MAP-2 or the astrocyte-specific protein GFAP, as indicated.

(B) RT-PCR demonstrating specific expression of specific AcP isoforms in lentiviral vector-transduced neuronal cultures but not in nontransduced *AcP*$^{-/-}$ culture 2 days after transduction.

(C) RT-PCR detection of *Ccl2* transcript in transduced neuronal cultures stimulated for 4 or 18 hr with IL-1β (10 ng/mL), as indicated.

(D) Gene intensity profiles of AcP-deficient and AcP isoform-reconstituted neuronal cultures (as indicated) stimulated with IL-1β (10 ng/mL) for 4 hr. RNA samples were used to hybridize a 45,000 probe set microarray as described in the Experimental Procedures. Immunohistochemistry images representative of several independent cultures and microarray experiment performed once with triplicate stimulations for each cell population.

AcPb-deficient mice bred normally and were phenotypically normal. Staining of brain sections from 8-week-old AcP- or AcPb-deficient mice with Weil (to reveal myelin) and Thionine Nissl (to reveal cell bodies) did not reveal obvious abnormalities as compared to age- and gender-matched wild-type controls (Figure 6C). We next demonstrated that peripheral responsiveness to IL-1 was still intact in AcPb-deficient mice. IL-6 induction in response to IL-1 was observed in splenocyte cultures from three independent mice from both wild-type and AcPb-deficient colonies (Figure 6D). In contrast, IL-1 was unable to induce IL-6 secretion from AcP-deficient splenocytes ($p < 0.01$), consistent with previous findings (Cullinan et al., 1998). All three cultures responded to LPS stimulation, indicating that cells from both knockouts were still responsive to an alternative form of activation. Taken together, our results indicate that the AcPb exon 12b deletion selectively ablated the AcPb isoform while maintaining classic AcP expression and function.

Effects of Pan-AcP and AcPb-Specific Deletion in Models of CNS Inflammation

We examined the effect of complete AcP deficiency versus AcPb-specific deletion in two different models of immune-mediated CNS pathology. First, we evaluated both mutant strains in experimental autoimmune encephalomyelitis (EAE), a model of peripherally induced autoimmune-mediated CNS disease. Subcutaneous immunization with MOG_{35-55} in CFA resulted in 100% disease incidence in wild-type C57Bl/6 mice (Figure 7A). In contrast, AcP-deficient mice were almost completely protected from disease with only 5% incidence (1 of 18 mice) and significantly less weight loss and lower clinical score compared to wild-type mice (Figures 7A–7C). AcPb-deficient mice, however, had disease onset and incidence (Figure 7A) and disease progression (Figures 7B and 7C) similar to that of wild-type controls. Nevertheless, 11 days after immunization, the AcPb-deficient mice did have a statistically significant increase in weight loss compared to wild-type controls ($p < 0.05$) (Figure 7B). We measured mRNA expression of several inflammatory mediators in the spinal cords of naive mice and mice at 20 days after immunization. MOG_{35-55} immunization led to significantly elevated amounts of IL-1β and TNF mRNA in the spinal cords of wild-type mice compared to naive animals (Figure 7D). IL-1β and TNF were comparably increased in the spinal cords of immunized AcPb-deficient mice, but not in AcP-deficient mice, compared to the respective naive controls, and these results correlated with the disease status. We also observed evidence of T cell-driven CNS inflammation, including increased amounts of the mRNA for Th1-associated

Table 1. Two Classes of AcP-Dependent Responses

Gene Name	Accession #	AcP (p value)	AcP+AcPb (p value)
AcP-Dependent Responses Unaffected by AcPb Expression			
Gbp2	NM_010260	36.8 ± 13% (0.0)	38.5 ± 22% (8.0E-24)
Ccl2	NM_011333	14.1 ± 19% (2.2E-17)	13.6 ± 14% (6.2E-27)
Cxcl2	NM_009140	13.6 ± 21% (5.4E-14)	12.7 ± 29% (3.0E-08)
Ptx3	NM_008987	11.7 ± 9% (0.0002)	11.9 ± 13% (0.0004)
Cxcl5	NM_009141	10.0 ± 27% (2.5E-07)	8.8 ± 22% (5.4E-09)
Egr2	NM_010118	8.8 ± 14% (2.0E-28)	8.1 ± 13% (2.8E-31)
Tlr2	NM_011905	5.2 ± 13% (7.9E-14)	5.0 ± 14% (5.9E-10)
AcP-Dependent Responses Attenuated by AcPb Expression			
Atf3	NM_007498	22.4 ± 37% (1.6E-08)	3.8 ± 19% (0.00005)
Tnfrsf12a	NM_013749	39.3 ± 50% (1.3E-12)	1.9 ± 29% (4.3E-08)
Cebpd	NM_007679	12.7 ± 9% (0.0)	4.1 ± 14% (1.8E-08)
Cp	NM_001042611	10.1 ± 14% (5.1E-20)	2.5 ± 22% (0.01)
Fos	NM_010234	2.9 ± 7% (2.2E-13)	1.5 ± 7% (0.0008)

Fold-change induction for each gene was measured in a ratio between sets of chips from triplicate samples of unstimulated and IL-1β-stimulated neuronal cultures with the Resolver log error converted to an average percentage. The p value in parentheses is evaluated for the null hypothesis of no change because of stimulation and is uncorrected for multiple testing. The second column is the IL-1 induced fold-change in AcP-deficient cells transduced with only the AcP vector, whereas the third column is for cells transduced with both AcP and AcPb vectors.

transcription factor T-bet and the effector cytokine IL-17A, in immunized wild-type and AcPb-deficient mice but not the AcP-deficient mice, compared to naive mice. Taken together, these results indicate that the absence of AcP is associated with profound protection from EAE, whereas loss of AcPb does not confer the same protection.

Innate immune activation in the brain is not itself detrimental but can lead to neurotoxic consequences if not adequately regulated, such as, for example, in the context of glucocorticoid blockade. In such a model, it has been shown that the ensuing neurodegeneration in response to a single intracerebral bolus of LPS is in part dependent on IL-1, suggesting that in the absence of sufficient regulation of IL-1 activity, signaling can lead to neuronal loss (Nadeau and Rivest, 2003). We used this experimental system to determine whether the regulatory effect of AcPb expression is associated with neuroprotection in the context of a local inflammatory response. LPS was infused into the brains of wild-type, AcP-, or AcPb-deficient mice (3–4 mice/group), and subsequent inflammatory response and neuronal damage was assessed by in situ hybridization for expression of IL-1β and the myelin constituent PLP, respectively, or by Fluoro-Jade (FJB) staining of degenerative neurons. Consistent with previous findings, LPS was shown to induce an inflammatory response in the brain as evidenced by induction of IL-1β mRNA within 24 hr, which was similar in all three lines of mice (Figure 7E). IL-1β mRNA was undetectable in the saline-treated animals (not shown). As shown in Figures 7F–7H, LPS administration did not lead to observable demyelination or neuronal loss in either wild-type or AcP-deficient animals. In contrast, at day 3, AcPb-deficient mice exhibited a clear and localized loss of expression of the myelin constituent PLP that was near, but distinct from, the LPS injection site. This decrease in PLP mRNA expression was frequently associated with a concomitant neurodegeneration, demonstrated by FJB-bright neuronal bodies at the site of PLP loss in AcPb null brains. The physical injury of the needle also induced some FJB-positive neurons near the injection tract in both saline- and LPS-treated groups of all mice; however, FJB-positive neurons were found far from the injection site only in the brains of all AcPb-deficient mice challenged with LPS and none of the wild-type or AcP-deficient mice. Interestingly, the LPS-induced neuronal loss in AcPb mice was not yet detectable at 24 hr (not shown), suggesting that it was not an immediate consequence of LPS administration. These results indicate that AcPb can play an important role in neuro-protection during an acute inflammatory response in the CNS, possibly by regulating the activity of IL-1.

DISCUSSION

IL-1 and the IL-1 receptors are expressed in the brain, and IL-1 is known to regulate a number of adaptive physiologic processes in the CNS, including sickness behavior (Konsman et al., 2002), fever response (Dinarello, 2004), and activation of the pituitary-adrenal axis (Besedovsky et al., 1986). Many of these activities are thought to result from direct effects of IL-1 on neuronal cells. IL-1 expression in the brain is usually low and exogenous IL-1 is not itself toxic to neurons when administered acutely into the healthy brain. Cellular responses to IL-1 are modulated by the physiologic state, however, and under various pathological conditions IL-1 has been shown to exacerbate neurodegeneration, for example, in response to traumatic brain injury, seizure, or acute ischemic insult (reviewed by Bartfai et al., 2007; Rothwell et al., 1997). Unregulated IL-1 activity has also been implicated in mental retardation associated with multisystem inflammatory disease (Goldbach-Mansky et al., 2006). The mechanisms by which IL-1 influences these centrally mediated effects are likely to be complex and may involve, in part, neuronal-specific signaling (Davis et al., 2006; Pizzi et al., 2002; Srinivasan et al., 2004; Tsakiri et al., 2008). The existence and structure of the AcPb molecule suggests that it could play

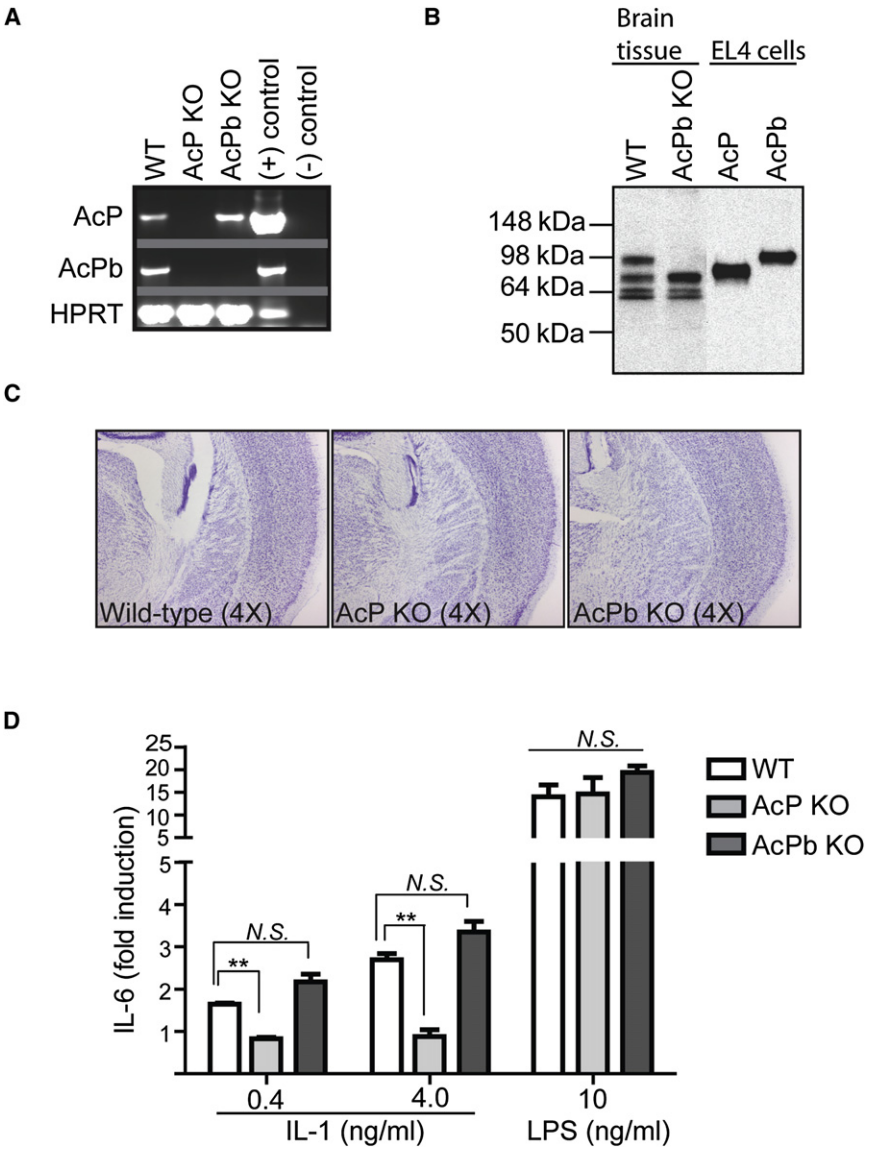

Figure 6. Generation of AcPb Knockout Mouse

AcPb-deficient (KO) animals were generated as described in the Experimental Procedures and as indicated in Figure 1.

(A) RT-PCR primers specific for AcP, AcPb, or HPRT (as a control) were used to amplify cDNA generated from whole brain tissue from wild-type, AcP-deficient, or AcPb-deficient mice. Plasmid DNA for each cDNA was used as positive PCR controls and H_2O as a negative PCR control. Data representative of at least three mice per genotype.

(B) Immunoprecipitations of AcP- and AcPb-EL4 cell lysates or whole brain lysates from wild-type or AcPb-deficient mice were performed with a pan-AcP antibody and analyzed by immunoblot with a polyclonal AcP antibody, as described in the Experimental Procedures. Data representative of duplicate independent experiments.

(C) Brains were collected from 10-week-old mice and coronal plane sections were stained with Thionine- Nissl to reveal cell bodies and general morphology. Images are indicative of observations across the interval of sections. Data representative of three age-matched mice per genotype.

(D) Splenocytes were isolated from wild-type, AcP-deficient, or AcPb-deficient mice and stimulated with IL-1β at the indicated concentrations. Supernatants were collected for determination of IL-6 concentrations after 48 hr. Graph shows mean ± SEM, n = 2 and results were generated with splenocytes from three individual mice per genotype and average fold induction is indicated (N.S. = not significant, $^{**}p < 0.001$).

a role in determining specific IL-1-dependent outcomes in the CNS.

AcPb was recruited to ligand-bound IL-1 receptor in similar fashion to AcP and we presume that AcPb can also be recruited to other AcP-utilizing receptors such as ST2 (Ali et al., 2007; Chackerian et al., 2007; Palmer et al., 2008) and IL-1Rrp2 (Towne et al., 2004) once they have bound their ligands. IL-1Rrp2 was initially cloned from brain (Lovenberg et al., 1996) and ST2 mRNA is found in the CNS (unpublished observations and Andre et al., 2005), so the functions of these two receptors and their ligands IL-33 and the IL-1F proteins may also be modified by AcPb. AcPb does not permit the recruitment of key signaling molecules or the elicitation of canonical signaling responses whether either IL-1α or IL-1β is used or when AcPb is coexpressed with chimeric receptors containing the cytoplasmic domains of other IL-1R family members (not shown); thus the signaling function, if any, of AcPb is considerably different from that of AcP. It is likely that the inability to recruit key signaling components to the receptor and promote cytokine induction is due to the changed configuration in the DD loop and αD helix regions of the AcPb TIR domain and to the altered charge distribution pattern on its surface, both of which could affect interaction with other proteins. It is interesting to note that SIGIRR, another TIR domain-containing transmembrane protein postulated to play a negative role in IL-1 and TLR signaling (Garlanda et al., 2007; Qin et al., 2005; Thomassen et al., 1999; Wald et al., 2003), also has several prolines in the same region as those which disrupt the αD helix in AcPb.

In contrast to AcP, introduction of AcPb into neuronal cultures derived from mice deficient in all splice forms of AcP led to only a low-level induction of a limited set of genes, of perhaps questionable significance. This result indicated that even if AcPb interacts with novel cofactors or utilizes distinct signal transduction pathways, it is still unable to mediate a robust IL-1 response at the level of gene induction. In the context of AcP and AcPb coexpression, genes induced by IL-1 fell into one of two categories. Some genes (e.g., *Gbp2*, *Ccl2*, and *Cxcl2*) were induced as strongly in coexpressing cells as in cells expressing only AcP. Expression of other genes (e.g., *Atf3*, *Icam1*, and *Cebpd*), however, was dramatically inhibited when AcPb was coexpressed with AcP. Thus, consistent with its retention of a variant

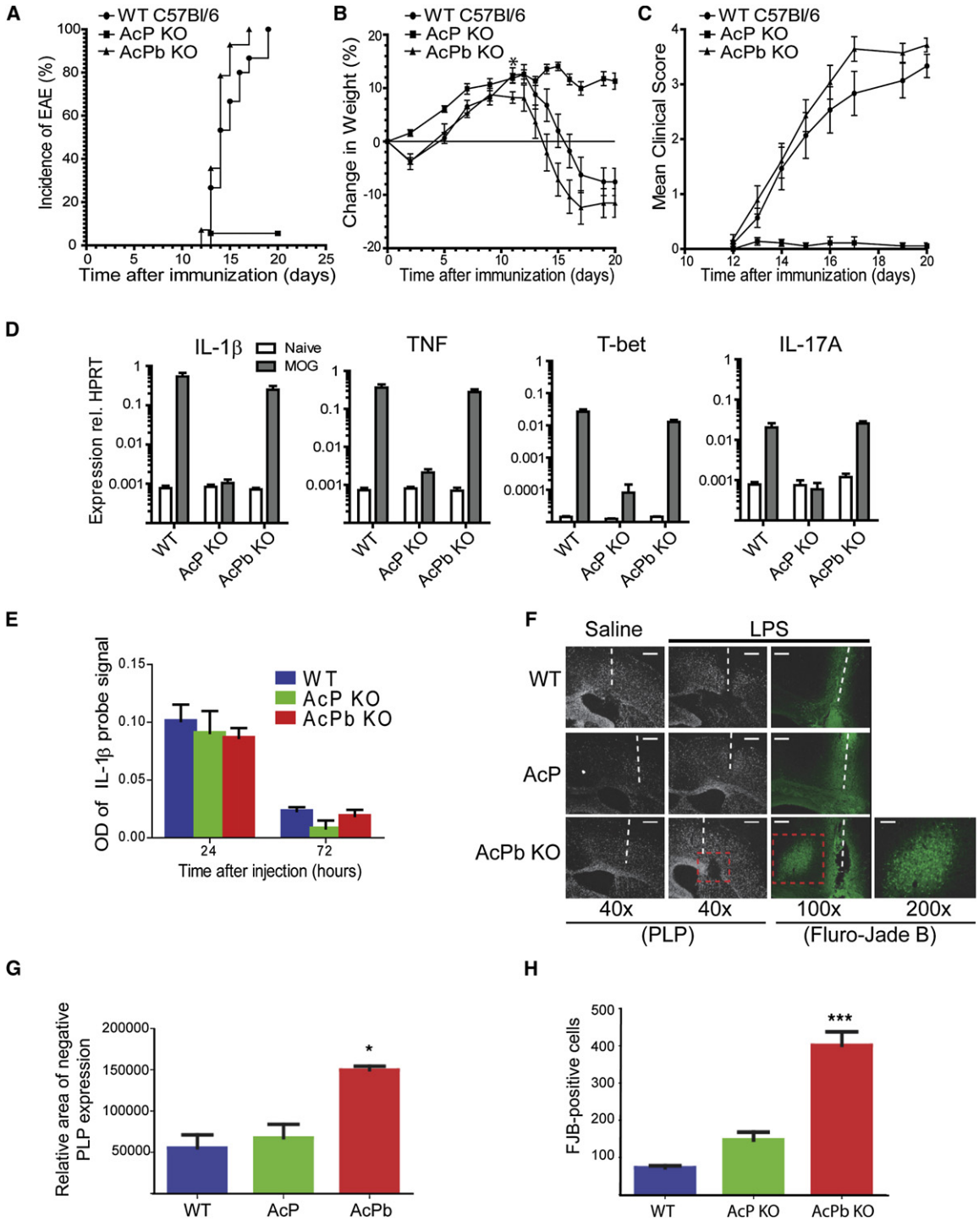

Figure 7. Effect of AcP and AcPb Deletion In Vivo

Female C57Bl/6 wild-type, AcP-deficient (AcP KO), or AcPb-deficient (AcPb KO) mice (approximately 10 weeks old) were immunized s.c. with MOG_{35-55} in CFA on day 0 to induce experimental autoimmune encephalomyelitis. Pertussis toxin (350 ng/mouse) in PBS was injected i.v. 48 hr after immunization. Animals were monitored, weighed, and scored for clinical disease every other day until disease was observed, then daily thereafter.

(A) Disease incidence ($p < 0.0001$, Logrank test).

(B) Change in weight ($p < 0.05$, one-way ANOVA, Tukey's post hoc test).

(C) Clinical score.

(D) RNA was extracted on day 20 after immunization from spinal cords of mice from each strain as indicated and gene expression was profiled by real-time PCR. Gene expression relative to HPRT is plotted for each gene as mean ± SEM. Experiment performed once with 5 mice per genotpye.

TIR domain, AcPb is not a general inhibitor of IL-1 function, but rather changes the quality of the IL-1 response by skewing the gene expression pattern. Another report has described this same splice variant of AcP (Lu et al., 2008), but the results reported in that manuscript for the effect of the AcP variant on gene expression differ from ours. We do not know how to explain the discrepancy except that their conclusions were drawn predominantly from overexpression studies in HEK293 cells.

It was previously reported that IL-1R deficiency protects mice from Th17 cell-mediated inflammation and CNS damage in a model of EAE (Sutton et al., 2006). Consistent with these findings, we observed a profound protective effect of AcP deficiency in EAE; however, the loss of AcPb conferred no such protection compared to wild-type controls, possibly reflecting the contribution of a peripheral immune compartment in this model. Inhibition of IL-1 directly in the CNS has been shown by others to be beneficial in EAE; however, this may have been due to inhibiting actions of IL-1 on non-AcPb-expressing cells (Furlan et al., 2007). In an acute model of local LPS challenge in the CNS, the absence of AcPb expression led to neuronal loss in response to an otherwise nontoxic innate immune stimulation. This in vivo result indicated that, possibly by modulating the intracellular signaling and gene expression response to LPS-induced IL-1, AcPb expression may buffer the neurotoxic effects of IL-1 or possibly the other AcP-utilizing cytokines. Interestingly, the transcription factor ATF3, one of the IL-1-induced genes whose induction was dramatically reduced by AcPb coexpression in our neuronal culture, has been implicated in mediating neurodegeneration in various experimental settings (Chen et al., 2008; Song et al., 2008). In light of this finding, it will be interesting to further investigate how different environmental and pathologic conditions modulate the relative expression of AcP and AcPb, because their ratio could determine neuronal outcome in settings that involve excess IL-1 activity.

The presence of AcPb extends the range of regulatory mechanisms used to control IL-1 activity. In addition to the blockade of the type I IL-1 receptor by IL-1ra and the decoy function of either membrane-bound or soluble type 2 IL-1R, there are now three regulatory complexes involving the accessory protein. Soluble AcP greatly enhances the ability of soluble type 2 IL-1R to inhibit IL-1 action (Smith et al., 2003), and on the cell membrane, full-length type 2 IL-1R bound to IL-1 decoys not only the ligand but also AcP away from productive interaction with IL-1 bound type 1 IL-1R (Lang et al., 1998; Malinowsky et al., 1998). There is also an inhibitory activity of soluble AcP alone although the mechanism has not been biochemically defined (Smeets et al., 2005). In contrast to these forms of regulation, only certain IL-1 responses are inhibited by AcPb. Thus, rather than eliminating an IL-1 signal entirely, the quality of the signal is altered. One hypothesis for the selective inhibitory effect of AcPb is that it generally inhibits all IL-1 responses in an AcP-competitive manner through a failure to recruit MyD88 and IRAK4, and that the effect on expression of particular genes is determined by the overall strength of signal required for induction of each gene, such as previously described for Erk-dependent activation of IL-1 and TNF genes (Papoutsopoulou et al., 2006). Our preliminary experiments do not support this hypothesis. Another explanation would be that AcPb initiates a signaling function that is insufficient for gene induction on its own, but might be required for full induction of some genes, possibly in association with novel adaptor proteins expressed in the brain (Kim et al., 2007; Su et al., 2007). A third possibility is that the functional IL-1 receptor complex contains multiple IL1R and AcP molecules, and if AcPb as well as AcP is part of the complex but is unable to recruit MyD88, the stoichiometry of the signaling complex would be altered.

In addition to its altered TIR domain, AcPb differs from AcP in that it contains a C-terminal "tail" of approximately 140 amino acids. C-terminal tails are also found in the IL-1R family members SIGIRR, TIGIRR, and IL-1RAPL (TIGIRR-2); however; the amount of sequence identity among them is low and none are homologous to the AcPb sequence. Although this has obvious implications for regulation of signaling, we have found that the presence or absence of the C-terminal tail does not affect the inability of AcPb to mediate IL-1-IL-1R signaling (not shown). The C-terminal tail could of course mediate a function entirely independent of IL-1 signaling. In the case of the X-linked receptor family member APL, which is genetically associated with cognitive function and autism in humans, the C-terminal extension is reported to interact with neuronal calcium sensor-1 and regulate neuron growth (Bhat et al., 2008; Gambino et al., 2007; Gao et al., 2008; Piton et al., 2008; Tabolacci et al., 2006). The C-terminal extension of AcPb offers the opportunity to interact with other proteins, recruiting them to the receptor complex or perhaps affecting the cellular location of the complex.

EXPERIMENTAL PROCEDURES

cDNA Cloning

A computational search for novel sequences with similarity to members of the IL-1R family was applied to human genomic DNA sequence (Celera human genome assembly R23- sequence CRA27000022534528). An open reading frame was identified on chromosome 3q28 that was 31% identical to exon 12 of IL-1RAcP. 5′ RACE and PCR were used to clone full-length AcPb sequence from human cDNA libraries. An orthologous AcPb exon 12 was identified in mouse genomic sequence that is 92.4% identical to the human exon at the amino acid level and full-length AcPb cDNA was cloned from mouse total brain.

PCR

First-strand cDNA from multiple human and mouse tissues was amplified by real-time PCR via Taqman primer and probe sets specific for AcP or AcPb. The sequences of the primers and probes are as follows (5′ to 3′). Human AcP: primer 1 (GGGCAGGTTCTGGAAGCA) at 900 nM, primer 2

(E) Mice (approximately 10 weeks old) were anesthetized and 1 μl of LPS (1 μg/μl) was injected intracerebrally over a 1 min period. 3 days later, mice were deeply anesthetized and perfused, and fixed brains were collected and processed as described in the Experimental Procedures. IL-1β mRNA was quantified after LPS administration by in situ hybridization. OD = optical density of IL-1β signal on radiographic film (not shown).

(F) Proteolipid protein (PLP) in situ hybridization (black and white image) and Fluoro-Jade B (FJB) staining (cell bodies of degenerating neurons stain green) of brains 3 days after LPS administration. White dashed lines indicate location of injection tract and red dashed boxes indicate regions of localized PLP loss and FJB-positive neurons (also shown at 200× magnification from AcPb brain).

(G and H) The relative area of lost PLP expression (G) or the number of FJB-positive degenerating neurons (H) were quantified by ImageJ software and results are expressed as mean ± SEM (*$p < 0.05$, ***$p < 0.001$). Data are representative of brains from either 3 or 4 individual mice per treatment group.

(GCTAGACCGCCTGGGACTTT) at 900 nM, and FAM probe (TCACTGGCA TGGCCACCTGCAG) at 200 nM. Human AcPb: primer 1 (TCCAAGCACCGAG GGAAGT) at 900 nM, primer 2 (AGGTGATTCTCTCCTTCACAGTAGGT) at 900 nM, and FAM probe (CCGCCACCTGCCGCTGTTG) at 200 nM. Mouse AcP: primer 1 (GGGCAACATCAACGTCATTTT) at 300 nM, primer 2 (CAGCTC TTTCACCTTCATGTCCTT) at 50 nM, and FAM probe (CACAGCTTTGTACTGC ACT) at 200 nM. Mouse AcPb: primer 1 (GGAGTTTAAGCTGGGTGTCATGT) at 50 nM, primer 2 (TGCTCAAGCGGACGGTACT) at 50 nM, and FAM probe (CCATTGCCACTAAGC) at 200 nM. All reactions were run in triplicate, and Ct (threshold) values to determine relative expression were normalized against the housekeeper gene HPRT. cDNAs from pooled human brain regions were obtained from Clontech. Real-time PCR profiling of spinal cord tissue from mice with EAE was performed with a custom Taqman Low density Array (Applied Biosystems). For RT-PCR analysis of AcP and AcPb expression in cultured cells, day 16 embryonic mouse hippocampal neurons and astrocytes were cultured as previously described (Srinivasan et al., 2004). Total RNA was isolated with trizol reagent (Invitrogen) as recommended by the manufacturer and 1 μg of reverse-transcribed cDNA was amplified for 35 cycles with the following primers: AcP (mAcP.cyto.foward 5′-TGTTTCCTATGCAAGAAATGT GGAAGAAGAGG-3′, mAcP.cyto.rev: 5′-TGCTTGTCATTGCTAGACCACCTG G-3′) and AcPb (mAcP.cyto.foward: 5′-TGTTTCCTATGCAAGAAATGTGGAA GAAGAGG-3′, mAcPb.1.rev: 5′-ATGGGGTTGCTCAAGCGACGGTACTCCA C-3′). PCR products were resolved on a 1% agarose gel and stained with ethidium bromide.

In Situ Hybridization

Antisense ^{35}S-UTP riboprobes specific for mouse AcP or AcPb mRNAs were made with RNA polymerase reactions with linearized plasmids containing either mouse AcP exon 12 or AcPb exon 12. Adult mouse brain sections were hybridized and exposed to radiographic emulsion for 5 or 12 days. As a control, sense strand riboprobe hybridizations were performed. Sections were stained with hematoxylin and eosin for bright field images.

Computational Modeling

The models of AcP and AcPb TIR domains were built based on alignments to the crystal structure of the Toll/Interleukin-1 receptor (TIR) domain of human IL-1RAPL (Khan et al., 2004), PDB id 1T3G, chain A. The protein structure models were built via the Homology Modeling method within the Molecular Operating Environment (MOE, Chemical Computing Group, Montreal, Quebec, Canada).

EL4 Stable Lines

EL4.16a cells (IL-1R$^+$/AcP$^-$ mouse lymphoma line) were transduced with retroviral vectors (Amgen, Inc.) encoding full-length muAcP or muAcPb and selected by FACS sorting for positive surface expression of the AcP extracellular domain with M215 antibody (rat IgG, Amgen Inc.). For immunoprecipitation experiments, 3 × 10^7 cells were incubated with or without IL-1β (100 ng/mL) at 37°C for 3 min. Whole-cell lysates were immunoprecipitated with the M215 antibody then subjected to SDS-PAGE. Coprecipitation of IL-1R or signaling molecules was evaluated by western blotting with anti-muIL-1R, anti-MyD88, or anti-IRAK4 polyclonal antibodies (P2, Amgen Inc., Chemicon #16527 or #16529 and Cell Signaling Technologies #4363, respectively). For IL-2, IL-5, and IL-6 measurements, 0.25 × 10^6 cells were incubated in triplicate for 24 hr in the presence of 300 ng/mL ionomycin and 100 pg/mL PMA (both from Sigma) plus or minus IL-1β (100 pg/mL). Cytokine levels in the supernatants were quantified by Luminex-based multiplex assay (Luminex Corp.) with reagents from Biosource International. To measure induction of phosphorylated kinases, 2.0 × 10^7 cells were incubated with or without IL-1β (10 ng/mL) or 0.5 M sorbitol at 37°C for various lengths of time and then immediately lysed. Equivalent amounts of lysates (approximately 0.4 × 10^6 cell equivalents/lane) were subjected to SDS-PAGE and western blotting was performed with phospho-specific antibodies phospho-p44/p42 (Cell Signaling Technologies #9101), phospho-JNK (Cell Signaling Technologies #9251), and phospho-p38 (Cell Signaling Technologies #9211).

Animals Used and Description of AcPb Knockout Mice

Homozygous AcP-deficient mice (B6;129S-*Il1rap*) were obtained from Taconic Laboratories and were completely backcrossed onto a C57BL/6Tac background as confirmed by microsatellite analysis (performed by Charles River Laboratories). AcPb knockout mice (B6;129-*Il1racpb*) were generated utilizing a 10.6 kb targeting cassette that replaced the entire AcPb-specific exon 12 with a neomycin resistance gene (as shown in Figure 1). The upstream exon 12 of classic AcP and the intervening 7.3 kb intron were left intact in order to maintain expression of normal full-length AcP. 129 embryonic stem (ES) cells were transfected with the targeting vector and selected under standard conditions. ES cell clones were transplanted into Black-Swiss females and homozygous animals were backcrossed completely onto a C57BL/6Tac background, as confirmed by microsatellite analysis (performed by Charles River Laboratories). *Il1racpb* mice bred normally and appeared phenotypically normal. Wild-type and knockout mice were subsequently obtained from Taconic Labs, where they were maintained under standard germ-free barrier conditions. All animal studies were reviewed and approved by the Amgen Animal Care and Use Committee or were conducted according to the Canadian Council on Animal Care guidelines, as administered by the Laval University Animal Welfare Committee.

Cortical Neuron Cultures

Pregnant mice (E17–E18) were anesthetized by CO_2 and brains were surgically removed. Microdissected cortical tissue was digested for 45 min at 37°C in papain solution (Worthington Biochemical) then gently disassociated in DMEM + 10% FBS with a 10 ml pipette followed by gentle filtration through a 40 μm cell strainer. Single-cell suspensions were plated into 6-well tissue culture dishes precoated with 0.1 mg/ml Poly-L-Ornithine (Sigma) and placed in a 37°C incubator with 5% CO_2 (approximately 1 × 10^6 cells/well). 30 min later, the medium was replaced with serum-free neuronal growth medium (2% B-27 supplement + 1% PSG in Neurobasal Medium [Invitrogen Corp]) and cultures were maintained for 9 days to allow for neuronal maturation. For immunostaining, cells were fixed for 15 min with 2% paraformaldehyde then permeabilized with 0.1% Triton. Cells were blocked with SuperBlock (Pierce) and 2.5% normal horse serum (Hyclone) for 1.5 hr then incubated with primary antibodies diluted in TBS + 1% horse serum + 0.05% Tween-20. For neuronal staining: anti-MAP-2 (Chemicon Ab5622), for glial cell staining: anti-GFAP (Chemicon MAB3402). Staining was completed with NovRed substrate and reagents from the Vectastain ABC peroxidase system (Vector Laboratories). AcP or AcPb expression and induction of CCL2 mRNA was determined by RT-PCR analysis of total RNA.

Microarray Analysis

Cortical neuron cultures were established from homozygous AcP-deficient mice (B6;129S-*Il1rap*) (Cullinan et al., 1998) as described above. After 7 days of culture, cells were transduced at an MOI of 5 with lentivirus vector (pLV401, Amgen Inc.) engineered to express either a cytoplasmic domain-truncated form of IL-2Rα (CD25, control) or full-length muAcP or muAcPb. After incubation for 2 hr at 37°C, cells were washed with PBS and placed back in Neurobasal growth medium and cultured for 2 days. On day 9, cells were left untreated or stimulated in triplicate with IL-1β (10 ng/mL) for either 4 or 16 hr and then collected for total RNA preparation. Receptor expression and *Ccl2* induction was confirmed by RT-PCR and for microarray analysis, individual biological replicate RNAs were separately labeled and hybridized to Affymetrix Mo430 microarray chips containing approximately 45,000 probe sets (Affymetrix). Data from individual arrays were first normalized then compared as ratios between sample sets at the level of the reporter probes, generating an error-weighted gene expression ratio via the Resolver software system (Rosetta Biosoftware). Sequences with high noise between replicate experiments were filtered out, and expression changes were calculated with the Resolver "Affymetrix with Reporters" error model. Relative error was calculated in logarithmic space and converted to a mean error in Fold-Change.

Characterization of Mutant Mice

To examine the expression of AcP and AcPb in mutant mice, whole brains were isolated from wild-type, AcP-deficient, and AcPb-deficient animals and total RNA was evaluated by RT-PCR amplification of AcP, AcPb, and the control gene HPRT. Phenotypic analysis of age-matched brains was assessed by Weil and Thionine staining to reveal cell bodies and myelin, respectively (Neuroscience Associates, Knoxville, TN). In brief, brains were perfused, embedded, and sectioned at 35 μm in the coronal plane through the entire

brain. Staining was evaluated at 840 μm intervals. To measure the responsiveness of peripheral cells to IL-1β, spleens were harvested from individual C57Bl/6, AcP-deficient, and AcPb-deficient mice (n = 3/group) and RBC-free single cell cultures were established. Cells were left untreated or stimulated with hIL-1β (at 0.4 or 4.0 ng/ml) or LPS (10 ng/ml). Supernatants were collected 48 hr later and the concentration of IL-6 produced was determined by ELISA (R&D Systems). To examine expression of AcP protein isoforms in total brain, protein lysates were generated by homogenization of brain tissue in TPER lysis buffer (Pierce) via a TissueLyzer system (QIAGEN). Cleared lysates were immunoprecipitated at 4°C with anti-muAcP (M215) and proteins were subjected to SDS-PAGE, transferred to nitrocellulose membranes, and incubated overnight with a rabbit polyclonal antibody against muAcP that detects both AcP and AcPb (P2, Amgen Inc.). Similar M215 immunoprecipitations of AcP and AcPb from stable EL4 cell lines (described above) were included as controls on the gel. In brief, lysates were generated from 100 million cells in 3.2 ml of lysis buffer and AcP and AcPb were immunoprecipitated from 1 ml of lysate during an overnight incubation at 4°C with the M215 Ab, as above. Immunoprecipitated proteins, corresponding to approximately 6 million cell equivalents, were analyzed by immunoblot alongside the brain immunoprecipitations.

EAE

To induce EAE, 10-week-old female C57Bl/6 (n = 15), AcP-deficient (n = 18), and AcPb-deficient (n = 14) mice were immunized s.c. with 150 μg myelin oligodendrocyte glycoprotein amino acids 35–55 (MOG_{35-55}; Amgen Inc., Seattle, WA) in an emulsion with CFA (Sigma, St. Louis, MO) containing 400 μg *M. tuberculosis* H37 Ra (Difco Lawrence, KS) on day 0. Pertussis toxin (350 ng/mouse) in PBS was injected i.v. 48 hr after immunization. Animals were monitored, weighed, and scored for clinical disease every other day until disease was observed, then daily thereafter. Disease onset was defined as a score of 1 or more for more than two successive days. EAE scoring was performed as follows: 0, no abnormality; 1, a limp tail; 2, impairment of righting reflex or abnormal gait; 3, severe hind limb weakness, partial hind limb paralysis; 4, complete hind limb paralysis, mobile by use of forelimbs. Mice were euthanized on day 20 after immunization. Spinal cords from 5 naive mice and 5 immunized mice per group were harvested for real-time PCR low-density array analysis. GraphPad Prism 5.0 (GraphPad software Inc.) was used to determine statistical significance.

Intracerebral LPS Injection and Histology

Wild-type, AcP-deficient, and AcPb-deficient mice (approximately 10 weeks old) were acclimated to standard laboratory conditions at the CHUL Research Center (14 hr light, 10 hr dark cycle) with free access to rodent chow and water. Isofluorane was used to anesthetize the mice and the site for LPS injection was stereotaxically determined by microscopy. To reach the injection site, the coordinates from the bregma were −2 mm lateral and −3 mm dorsoventral. 1 μl of 0.9% NaCl solution or LPS (1.0 mg/ml) was injected for a period of 1 min via a microinjection pump (Razel Scientific Instruments, Stanford, CT). 1, 3, and 7 days later, mice were deeply anesthetized by i.p injection of a ketamine hydrochloride (91 mg/ml) and xylazine (9.1 mg/ml) solution. They were quickly transcardially perfused with a 0.9% saline solution followed by 4% paraformaldehyde/3.8% Borax solution (pH 9) at 4°C. Immediately after fixation, brains were removed from the skulls and post-fixed in 4% paraformaldehyde/3.8% Borax solution (pH 9) for 24 hr. After post-fixation, brains were placed overnight in a solution of 4% paraformaldehyde/3.8% Borax solution (pH 9) containing 10% sucrose. The brains were mounted on a microtome (Reichert-Jung, Cambridge Instruments Company, Deerfield, IL), frozen with dry ice, and sliced into 25 μm coronal sections from olfactory bulb to the end of the medulla. The obtained slices were placed in a cold cryoprotectant solution (0.5 M sodium phosphate buffer [pH 7.3], 30% ethylene glycol, 20% glycerol) and stored at −20°C. IL-1β and Proteolipid protein (PLP) mRNA expression was detected via in situ hybridization (ISH) as previously described (Laflamme et al., 1999) and neuronal cell death was characterized by Fluoro-Jade B (FJB) method (Nadeau and Rivest, 2003).

ACCESSION NUMBERS

The sequence for human AcPb has been deposited at GenBank (accession number FJ998418) and the sequence for mouse AcPb is identical to NM_001159318 (annotated as interleukin 1 receptor accessory protein, transcript variant 4). Microarray data are available as .CEL files at GEO under accession number GSE16104.

SUPPLEMENTAL DATA

Supplemental Data include two tables and can be found with this article online at http://www.cell.com/immunity/supplemental/S1074-7613(09)00229-5.

ACKNOWLEDGMENTS

H. Arnett provided helpful advice and discussion, M. Wiley and K. Christensen helped with knockout mice generation, and J. Scholler and C. Strathdee provided important technical support with lentiviral generation. H. Chen provided technical support of cortical neuron gene expression studies. M. Timour and D. Prosser performed the microarray experiments and B. Buetow helped perform phenotypic analysis of knockout brains. We are grateful to E. Magal and M. Zhang for excellent technical assistance with cortical neuron cultures. Finally, we thank E. Pinteaux (University of Manchester) for many useful suggestions. D.E.S., B.P.L., C.R., R.R.K., J.K., K.H., and J.E.S. are employees and shareholders of Amgen, Inc. S.R. is supported by the Canadian Institutes of Health Research and a Canadian Research Chair in Neuroimmunology.

Received: October 23, 2008
Revised: February 6, 2009
Accepted: March 17, 2009
Published online: May 28, 2009

REFERENCES

Ali, S., Huber, M., Kollewe, C., Bischoff, S.C., Falk, W., and Martin, M.U. (2007). IL-1 receptor accessory protein is essential for IL-33-induced activation of T lymphocytes and mast cells. Proc. Natl. Acad. Sci. USA *104*, 18660–18665.

Alpert, D., Schwenger, P., Han, J., and Vilcek, J. (1999). Cell stress and MKK6b-mediated p38 MAP kinase activation inhibit tumor necrosis factor-induced IkappaB phosphorylation and NF-kappaB activation. J. Biol. Chem. *274*, 22176–22183.

Andre, R., Lerouet, D., Kimber, I., Pinteaux, E., and Rothwell, N.J. (2005). Regulation of expression of the novel IL-1 receptor family members in the mouse brain. J. Neurochem. *95*, 324–330.

Bartfai, T., Sanchez-Alavez, M., Andell-Jonsson, S., Schultzberg, M., Vezzani, A., Danielsson, E., and Conti, B. (2007). Interleukin-1 system in CNS stress: Seizures, fever, and neurotrauma. Ann. N Y Acad. Sci. *1113*, 173–177.

Besedovsky, H., del Rey, A., Sorkin, E., and Dinarello, C.A. (1986). Immunoregulatory feedback between interleukin-1 and glucocorticoid hormones. Science *233*, 652–654.

Bhat, S.S., Ladd, S., Grass, F., Spence, J.E., Brasington, C.K., Simensen, R.J., Schwartz, C.E., Dupont, B.R., Stevenson, R.E., and Srivastava, A.K. (2008). Disruption of the IL1RAPL1 gene associated with a pericentromeric inversion of the X chromosome in a patient with mental retardation and autism. Clin. Genet. *73*, 94–96.

Blomer, U., Naldini, L., Kafri, T., Trono, D., Verma, I.M., and Gage, F.H. (1997). Highly efficient and sustained gene transfer in adult neurons with a lentivirus vector. J. Virol. *71*, 6641–6649.

Burns, K., Janssens, S., Brissoni, B., Olivos, N., Beyaert, R., and Tschopp, J. (2003). Inhibition of interleukin 1 receptor/Toll-like receptor signaling through the alternatively spliced, short form of MyD88 is due to its failure to recruit IRAK-4. J. Exp. Med. *197*, 263–268.

Chackerian, A.A., Oldham, E.R., Murphy, E.E., Schmitz, J., Pflanz, S., and Kastelein, R.A. (2007). IL-1 receptor accessory protein and ST2 comprise the IL-33 receptor complex. J. Immunol. *179*, 2551–2555.

Chen, H.M., Wang, L., and D'Mello, S.R. (2008). Inhibition of ATF-3 expression by B-Raf mediates the neuroprotective action of GW5074. J. Neurochem. *105*, 1300–1312.

Cullinan, E.B., Kwee, L., Nunes, P., Shuster, D.J., Ju, G., McIntyre, K.W., Chizzonite, R.A., and Labow, M.A. (1998). IL-1 receptor accessory protein is an essential component of the IL-1 receptor. J. Immunol. *161*, 5614–5620.

Davis, C.N., Mann, E., Behrens, M.M., Gaidarova, S., Rebek, M., Rebek, J., Jr., and Bartfai, T. (2006). MyD88-dependent and -independent signaling by IL-1 in neurons probed by bifunctional Toll/IL-1 receptor domain/BB-loop mimetics. Proc. Natl. Acad. Sci. USA *103*, 2953–2958.

Dinarello, C.A. (2004). Infection, fever, and exogenous and endogenous pyrogens: Some concepts have changed. J. Endotoxin Res. *10*, 201–222.

Furlan, R., Bergami, A., Brambilla, E., Butti, E., De Simoni, M.G., Campagnoli, M., Marconi, P., Comi, G., and Martino, G. (2007). HSV-1-mediated IL-1 receptor antagonist gene therapy ameliorates MOG(35–55)-induced experimental autoimmune encephalomyelitis in C57BL/6 mice. Gene Ther. *14*, 93–98.

Gambino, F., Pavlowsky, A., Begle, A., Dupont, J.L., Bahi, N., Courjaret, R., Gardette, R., Hadjkacem, H., Skala, H., Poulain, B., et al. (2007). IL1-receptor accessory protein-like 1 (IL1RAPL1), a protein involved in cognitive functions, regulates N-type Ca2+-channel and neurite elongation. Proc. Natl. Acad. Sci. USA *104*, 9063–9068.

Gao, X., Xi, G., Niu, Y., Zhang, S., Fu, R., Zheng, Z., Zhang, K., Lv, S., He, H., Xue, M., and Zhang, F. (2008). A study on the correlation between IL1RAPL1 and human cognitive ability. Neurosci. Lett. *438*, 163–167.

Garlanda, C., Di Liberto, D., Vecchi, A., La Manna, M.P., Buracchi, C., Caccamo, N., Salerno, A., Dieli, F., and Mantovani, A. (2007). Damping excessive inflammation and tissue damage in *Mycobacterium tuberculosis* infection by Toll IL-1 receptor 8/single Ig IL-1-related receptor, a negative regulator of IL-1/TLR signaling. J. Immunol. *179*, 3119–3125.

Goldbach-Mansky, R., Dailey, N.J., Canna, S.W., Gelabert, A., Jones, J., Rubin, B.I., Kim, H.J., Brewer, C., Zalewski, C., Wiggs, E., et al. (2006). Neonatal-onset multisystem inflammatory disease responsive to interleukin-1beta inhibition. N. Engl. J. Med. *355*, 581–592.

Huang, J., Gao, X., Li, S., and Cao, Z. (1997). Recruitment of IRAK to the interleukin 1 receptor complex requires interleukin 1 receptor accessory protein. Proc. Natl. Acad. Sci. USA *94*, 12829–12832.

Jiang, Z., Johnson, H.J., Nie, H., Qin, J., Bird, T.A., and Li, X. (2003). Pellino 1 is required for interleukin-1 (IL-1)-mediated signaling through its interaction with the IL-1 receptor-associated kinase 4 (IRAK4)-IRAK-tumor necrosis factor receptor-associated factor 6 (TRAF6) complex. J. Biol. Chem. *278*, 10952–10956.

Khan, J.A., Brint, E.K., O'Neill, L.A., and Tong, L. (2004). Crystal structure of the Toll/interleukin-1 receptor domain of human IL-1RAPL. J. Biol. Chem. *279*, 31664–31670.

Kim, Y., Zhou, P., Qian, L., Chuang, J.Z., Lee, J., Li, C., Iadecola, C., Nathan, C., and Ding, A. (2007). MyD88–5 links mitochondria, microtubules, and JNK3 in neurons and regulates neuronal survival. J. Exp. Med. *204*, 2063–2074.

Konsman, J.P., Parnet, P., and Dantzer, R. (2002). Cytokine-induced sickness behaviour: Mechanisms and implications. Trends Neurosci. *25*, 154–159.

Laflamme, N., Lacroix, S., and Rivest, S. (1999). An essential role of interleukin-1beta in mediating NF-kappaB activity and COX-2 transcription in cells of the blood-brain barrier in response to a systemic and localized inflammation but not during endotoxemia. J. Neurosci. *19*, 10923–10930.

Lang, D., Knop, J., Wesche, H., Raffetseder, U., Kurrle, R., Boraschi, D., and Martin, M.U. (1998). The type II IL-1 receptor interacts with the IL-1 receptor accessory protein: a novel mechanism of regulation of IL-1 responsiveness. J. Immunol. *161*, 6871–6877.

Li, C., Zienkiewicz, J., and Hawiger, J. (2005). Interactive sites in the MyD88 Toll/interleukin (IL) 1 receptor domain responsible for coupling to the IL1beta signaling pathway. J. Biol. Chem. *280*, 26152–26159.

Lovenberg, T.W., Crowe, P.D., Liu, C., Chalmers, D.T., Liu, X.J., Liaw, C., Clevenger, W., Oltersdorf, T., De Souza, E.B., and Maki, R.A. (1996). Cloning of a cDNA encoding a novel interleukin-1 receptor related protein (IL 1R-rp2). J. Neuroimmunol. *70*, 113–122.

Lu, H.L., Yang, C.Y., Chen, H.C., Hung, C.S., Chiang, Y.C., and Ting, L.P. (2008). A novel alternatively spliced interleukin-1 receptor accessory protein mIL-1RAcP687. Mol. Immunol. *45*, 1374–1384.

Malinowsky, D., Lundkvist, J., Laye, S., and Bartfai, T. (1998). Interleukin-1 receptor accessory protein interacts with the type II interleukin-1 receptor. FEBS Lett. *429*, 299–302.

Nadeau, S., and Rivest, S. (2003). Glucocorticoids play a fundamental role in protecting the brain during innate immune response. J. Neurosci. *23*, 5536–5544.

Palmer, G., Lipsky, B.P., Smithgall, M.D., Meininger, D., Siu, S., Talabot-Ayer, D., Gabay, C., and Smith, D.E. (2008). The IL-1 receptor accessory protein (AcP) is required for IL-33 signaling and soluble AcP enhances the ability of soluble ST2 to inhibit IL-33. Cytokine *42*, 358–364.

Papoutsopoulou, S., Symons, A., Tharmalingham, T., Belich, M.P., Kaiser, F., Kioussis, D., O'Garra, A., Tybulewicz, V., and Ley, S.C. (2006). ABIN-2 is required for optimal activation of Erk MAP kinase in innate immune responses. Nat. Immunol. *7*, 606–615.

Piton, A., Michaud, J.L., Peng, H., Aradhya, S., Gauthier, J., Mottron, L., Champagne, N., Lafreniere, R.G., Hamdan, F.F., Joober, R., et al. (2008). Mutations in the calcium-related gene IL1RAPL1 are associated with autism. Hum. Mol. Genet. *17*, 3965–3974.

Pizzi, M., Goffi, F., Boroni, F., Benarese, M., Perkins, S.E., Liou, H.C., and Spano, P. (2002). Opposing roles for NF-kappa B/Rel factors p65 and c-Rel in the modulation of neuron survival elicited by glutamate and interleukin-1beta. J. Biol. Chem. *277*, 20717–20723.

Qin, J., Qian, Y., Yao, J., Grace, C., and Li, X. (2005). SIGIRR inhibits interleukin-1 receptor- and toll-like receptor 4-mediated signaling through different mechanisms. J. Biol. Chem. *280*, 25233–25241.

Radons, J., Dove, S., Neumann, D., Altmann, R., Botzki, A., Martin, M.U., and Falk, W. (2003). The interleukin 1 (IL-1) receptor accessory protein Toll/IL-1 receptor domain: Analysis of putative interaction sites in vitro mutagenesis and molecular modeling. J. Biol. Chem. *278*, 49145–49153.

Rothwell, N., Allan, S., and Toulmond, S. (1997). The role of interleukin 1 in acute neurodegeneration and stroke: pathophysiological and therapeutic implications. J. Clin. Invest. *100*, 2648–2652.

Sims, J.E. (2002). IL-1 and IL-18 receptors, and their extended family. Curr. Opin. Immunol. *14*, 117–122.

Sims, J.E., and Smith, D.E. (2003). Regulation of interleukin-1 activity is enhanced by cooperation between the interleukin-1 receptor type II and interleukin-1 receptor accessory protein. Eur. Cytokine Netw. *14*, 77–81.

Smeets, R.L., Joosten, L.A., Arntz, O.J., Bennink, M.B., Takahashi, N., Carlsen, H., Martin, M.U., van den Berg, W.B., and van de Loo, F.A. (2005). Soluble interleukin-1 receptor accessory protein ameliorates collagen-induced arthritis by a different mode of action from that of interleukin-1 receptor antagonist. Arthritis Rheum. *52*, 2202–2211.

Smith, D.E., Hanna, R., Della, F., Moore, H., Chen, H., Farese, A.M., MacVittie, T.J., Virca, G.D., and Sims, J.E. (2003). The soluble form of IL-1 receptor accessory protein enhances the ability of soluble type II IL-1 receptor to inhibit IL-1 action. Immunity *18*, 87–96.

Song, D.Y., Yang, Y.C., Shin, D.H., Sugama, S., Kim, Y.S., Lee, B.H., Joh, T.H., and Cho, B.P. (2008). Axotomy-induced dopaminergic neurodegeneration is accompanied with c-Jun phosphorylation and activation transcription factor 3 expression. Exp. Neurol. *209*, 268–278.

Srinivasan, D., Yen, J.H., Joseph, D.J., and Friedman, W. (2004). Cell type-specific interleukin-1beta signaling in the CNS. J. Neurosci. *24*, 6482–6488.

Su, J., Richter, K., Zhang, C., Gu, Q., and Li, L. (2007). Differential regulation of interleukin-1 receptor associated kinase 1 (IRAK1) splice variants. Mol. Immunol. *44*, 900–905.

Sutton, C., Brereton, C., Keogh, B., Mills, K.H., and Lavelle, E.C. (2006). A crucial role for interleukin (IL)-1 in the induction of IL-17-producing T cells that mediate autoimmune encephalomyelitis. J. Exp. Med. *203*, 1685–1691.

Tabolacci, E., Pomponi, M.G., Pietrobono, R., Terracciano, A., Chiurazzi, P., and Neri, G. (2006). A truncating mutation in the IL1RAPL1 gene is responsible

for X-linked mental retardation in the MRX21 family. Am. J. Med. Genet. A. *140*, 482–487.

Thomassen, E., Renshaw, B.R., and Sims, J.E. (1999). Identification and characterization of SIGIRR, a molecule representing a novel subtype of the IL-1R superfamily. Cytokine *11*, 389–399.

Towne, J.E., Garka, K.E., Renshaw, B.R., Virca, G.D., and Sims, J.E. (2004). Interleukin (IL)-1F6, IL-1F8, and IL-1F9 signal through IL-1Rrp2 and IL-1RAcP to activate the pathway leading to NF-kappaB and MAPKs. J. Biol. Chem. *279*, 13677–13688.

Tsakiri, N., Kimber, I., Rothwell, N.J., and Pinteaux, E. (2008). Interleukin-1-induced interleukin-6 synthesis is mediated by the neutral sphingomyelinase/Src kinase pathway in neurones. Br. J. Pharmacol. *153*, 775–783.

Wald, D., Qin, J., Zhao, Z., Qian, Y., Naramura, M., Tian, L., Towne, J., Sims, J.E., Stark, G.R., and Li, X. (2003). SIGIRR, a negative regulator of Toll-like receptor-interleukin 1 receptor signaling. Nat. Immunol. *4*, 920–927.

Wesche, H., Henzel, W.J., Shillinglaw, W., Li, S., and Cao, Z. (1997a). MyD88: An adapter that recruits IRAK to the IL-1 receptor complex. Immunity *7*, 837–847.

Wesche, H., Korherr, C., Kracht, M., Falk, W., Resch, K., and Martin, M.U. (1997b). The interleukin-1 receptor accessory protein (IL-1RAcP) is essential for IL-1-induced activation of interleukin-1 receptor-associated kinase (IRAK) and stress-activated protein kinases (SAP kinases). J. Biol. Chem. *272*, 7727–7731.

Xu, Y., Tao, X., Shen, B., Horng, T., Medzhitov, R., Manley, J.L., and Tong, L. (2000). Structural basis for signal transduction by the Toll/interleukin-1 receptor domains. Nature *408*, 111–115.